

¹H NMR based metabolites analysis of murine melanoma cells and primary melanocytes

Yunxia Yang*, Shuyan Shen, Shihan Huang

School of Chemistry and Environmental Engineering, Yancheng Teachers University,
Yancheng, 224007, China

E-mail of the corresponding author: yangyx01@yctu.edu.cn

The research is financed by start-up grant (204060031) from Yancheng Teachers University, Jiangsu Higher Education Institutions of China (No. 22KJD180006).

Abstract

Melanoma is one of the most life-threatening skin cancer characterized by ineffective therapies and rising incidence. Here we applied ¹H NMR to acquire details of metabolic rewiring between primary melanocytes and murine melanoma cells. A total of 29 metabolites were assigned and identified. The principal component analysis (PCA) illustrated a distinct separation along the first component. A constructed orthogonal partial least squares-discriminant (OPLS-DA) model obtained intrinsic variations as PCA analysis did. The corresponding S-plot and loading plot revealed some significant variations of metabolites in melanoma compared with the control group, including the obvious increases of isoleucine, leucine, valine, 3-hydroxybutyrate, lactate, alanine, 2-oxoglutarate, glutathione, creatine, glycine, tyrosine, phenylalanine, histidine and remarkable decreases of lysine, acetate, n-acetyl-CH₃, n-acetyl cysteine, glutamine, glutamate, methionine, choline, taurine, glucose and formate. The down regulation of glucose and the accumulated lactate indicated enhanced aerobic glycolysis for energy requirements in melanoma cells. Decreased taurine acted to fight against reactive oxygen species, as evidenced by an active glutathione system in melanoma cells. Amino acid profiles altered different from any other cancer cells. Tumor-related amino acids identified by NMR might be helping advance the field of therapeutic intervention in melanoma.

Keywords: melanocytes, melanoma, NMR, multivariate analysis, pathway

DOI: 10.7176/JBAH/15-1-01

Publication date: January 30th 2025

1. Introduction

Melanocytes produce and store melanin to protect the cells against ultraviolet (UV) radiation and white light (Gordon, Mansur, & Gilchrest, 1989). Melanoma is the most aggressive skin cancer originating from melanocytes, which accounting for only 5% of all skin cancers while 80% of the deaths. Melanoma is curable if recognized and treated by surgical removal at the initial site. However, some patients remain high risk of recurrence after definitive surgery. As for other cancers, metastasis is considered the major threat to patient survival. Recent studies have shown that more than 90% melanoma patients get mutations in MAPK (Mitogen-Activated Protein Kinase) pathway, in which BRAF (B-Raf proto-oncogene, serine/threonine kinase), NRAS (NRAS proto-oncogene, GTPase) and NFI (Neurofibromatosis type 1) genes are mostly common changed (; Andersen et al., 1993; Curtin et al., 2005). To our knowledge, spatial and temporal information about specific metabolite increases and decreases also effectively complements gene expression and proteome studies, investigating metabolic alterations and identifying specific molecular biomarkers are critical for diagnosing patients and improving therapeutic efficiency in melanoma.

Cancer cells reprogram their metabolic pathways to synthesize an expanding biomass for dynamic stresses and proliferating (Colombino et al., 2012; Olivares, Däbritz, King, Gottlieb, & Halsey, 2015). Aerobic glycolysis was firstly observed in cancers by Otto Warburg in the 1920s (Cantor & Sabatini, 2012). The 'Warburg Effect' discovered that tumor relies on a high rate of glycolysis even under normal oxygen conditions, producing an

acidic extra-cellular environment (Warburg, Wind, & Negelein, 1927). Although clear mechanisms are still elusive, some evidences have shown that cell populations emerging from enhanced aerobic glycolysis get a significant growth superiority, as they alter surrounding acidosis environment to promote destruction of adjacent normal cells, acceleration of angiogenesis and degradation of the extracellular matrix their environment (Gatenby & Gawlinski, 1996; Vander Heiden, Cantley, & Thompson, 2009). Furthermore, glutamine is required to feed tricarboxylic acid cycle (TCA) as an alternative carbon source in tumors (Gatenby, Gawlinski, Gmitro, Kaylor, & Gillies, 2006; Zaidi et al., 2013). Malignant cells rapidly adapt to nutrient limitation by resetting their metabolism, another observation indicated that glucose-deprived melanoma cells heavily rely on acetate metabolism for survival (Cairns, Harris, & Mak, 2011). Despite a long and substantial history of study, the complex association between disturbed metabolism and uncontrolled proliferation remains an elusive area of investigation. Thus, understanding how melanoma cells obtain energy and maintain survival is essential for the establishment of appropriate therapies and diagnostic approaches.

Metabolomics allows the simultaneous and valid quantification of thousands of different metabolites within a biological system using sensitive and specific technologies (Lakhter et al., 2016). Nuclear Magnetic Resonance (NMR) provides an unbiased approach in a rapid and cost-effective manner. The analysis of NMR metabolomics datasets is typically conducted in two phases: spectral preprocessing and multivariate analyses including principal component analysis (PCA) and partial least-squares discriminant analysis (PLS-DA) methods which can be used to construct classification models or for biomarker discovery. Combined with statistical analysis, the growing accessibility of this approach is playing a substantial role in monitoring metabolic perturbations of endogenous low molecular weight metabolites, providing a new insight into physiological and pathological processes, the metabolic interactions, drug safety and efficacy assessment, disease diagnosis, and toxicity screening (Wishart, 2016). B16F10 cell line is one of the most used cell lines in melanoma originated from a tumor generated in C57BL/6 mice, representing a highly metastatic stage of melanoma (Sinclair et al., 2010). Up to now, several studies have compared metabolic profiles between melanoma and non-melanoma lesions in patients (Cillo, Dick, Ling, & Hill, 1987; Fedele, Galdos-Riveros, Jose de Farias e Melo, Magalhães, & Maria, 2013; Feng, Isern, Burton, & Hu, 2013), and metabolic profiling of human melanocyte and melanoma cell lines using GC-MS has been reported (Scott et al., 2011; Wang, Hu, Feng, Liu, & Hu, 2014). However, there is still no study concerning metabolites and relevant pathways alterations between primary melanocytes isolated from C57BL/6 mice and B16F10 melanoma cell lines with a same background.

The purpose of the study is to evaluate specific metabolic pathways associated with proliferative melanoma cells in attempting to identify the role of NAA for this terminal disease. An overall comparison of multiple metabolites allowed us to evaluate overall metabolic response characteristics of the two cell types. The results would provide new biomarkers and contribute to a deeper knowledge of the underlying molecular processes in melanoma.

2. Materials and Methods

2.1 Cell culture

B16F10 murine melanoma cells were obtained from Nanjing KeyGen Biology China (Nanjing, China). Primary melanocytes were isolated from C57BL/6 mice by Shanghai EK-Bioscience Biological Technology Co., Ltd (Shanghai, China). The two cells were cultured in complete RPMI 1640 medium (Sigma, St. Louis, MO) containing 10% fetal bovine serum, 100 IU/ml penicillin, and 100 µg/ml streptomycin. The cells were maintained in an incubator flushed with 5% CO₂ at 37 °C. The cell culture medium was refreshed every two days. Two cells were continuously observed by using the inverted microscope, for comparison of the cells morphology and proliferation.

2.2 Cell Metabolites Extraction and Preparation

Metabolites were extracted from cells in accordance with the reported protocols (Beckonert et al., 2007; Kim et al., 2017). Prior to metabolite isolation, cells were seeded in 60 mm diameter culture dishes with six independent replicates. Each sample contained about 5×10^6 cells. After 24 h, each dish was washed with 1 mL pre-cold PBS for three times, quenched with 2 mL ice-cold acetonitrile/water (1:1; v/v), and harvested with a cell scraper into a pre-cold Eppendorf tube in ice. Cell suspensions were homogenized and kept on ice for 10 min for better extraction before centrifugation at 12,000 g for 10 min at 4 °C. The aqueous acetonitrile extract solutions were frozen at -80 °C overnight and lyophilized under vacuum at -60 °C with a freeze dryer (BenchTop K, VirTis). The obtained extracts were stored at -80 °C for NMR analysis.

2.3 ¹H NMR Spectroscopy

All NMR protocols referred to M.H.Li et al (Cuperlovic-Culf, Ferguson, Culf, Morin, & Touaibia, 2012; Li et al., 2018), the dried residue was dissolved in 550 μ L D₂O phosphate buffer (0.2 M, pH 7.4) containing 0.05% (w/v) TSP as a referencing chemical shift (δ 0.0). After centrifugation at 12,000 g for 10 min at 4 °C, the clear supernatant was pipetted into a 5 mm bruker NMR tube.

NMR spectra were recorded on a Bruker AVANCE III 500 MHz NMR spectrometer at 298 K. A modified transverse relaxation-edited Call–Purcell–Meiboom–Gill (CPMG) sequence (90(τ -180- τ) n-acquisition) with a total spin-echo delay (2n τ) of 40 ms was used in the spectroscopy. ¹H NMR spectra were measured with 128 scans and collected into 32 K data points with a 10 000 Hz spectral width, and acquisition time of 3.28 s. In the end, Fourier transformation was applied to the spectra after multiplication of the FIDs (free induction decays) with an exponential weighting function corresponding to a line-broadening of 0.5 Hz.

2.4 Spectra Processing and Data Analysis

NMR spectra obtained were firstly processed using Bruker TopSpin software (version 2.1) with global phase correction, baseline correction and alignment. MestReC (3.7.4, Mestrelab Research SL) was used to export ¹H NMR spectra to ASCII files for importing into R software (<http://cran.r-project.org/>) to analyze data. Water signal and affected regions from 4.25 to 5.6 ppm were discarded before binning spectrum into 0.005 ppm width between 0.7 and 8.6 ppm for statistical analysis (Xing et al., 2018). The remaining spectra were normalized, mean-centered and pareto-scaled for further analysis.

Principal component analysis (PCA)-an unsupervised analysis method, was first implemented to get a general overview of the group classification. A supervised orthogonal partial least squares-discriminant analysis (OPLS-DA) was then performed to discard irrelevant systematic signals and pick up major features between two groups. The generated score plot showed the discrimination of categories, loadings plots and s-plot identified markedly altered metabolites that contributed to the discrimination. The validity of the models was repeatedly verified by two methods, a two-fold cross validation method and a 2000 times permutation test. The results were able to reveal the fitness and confirm the predictability of the supervised analysis comparatively.

2.5 Metabolites Peak Assignments and Statistical Analysis

Metabolites were assigned in accordance with online metabolome databases, such as Madison Metabolomics Consortium Database (MMCD) (De Meyer et al., 2008) and Human Metabolome Database (HMDB) (Cui et al., 2008), and verified by Chemomx NMR Suite 7.5 (Chemomx Inc., Edmonton, Canada). Two-dimensional NMR techniques TOCSY was also used to ensure metabolites assignments. Metabolites fold changes and associated p-values were calculated and corrected by BH (Benjamini Hochberg) method.

2.6 Pathway Analysis and Visualization

Potential biomarkers were assessed according to variable significance in the OPLS-DA model. Significantly altered metabolites and topology information were parsed into graph models using the KEGG database in metaboanalyst 4.0 pathway analysis-MetPA (www.metaboanalyst.ca) (Wishart et al., 2013). The schematic diagram of the overall metabolites and pathways affected in melanoma cells was visualized by ChemBioDraw Ultra 14.0.

3. Results

3.1 Morphological Characteristics of Cells

Representative morphology of primary melanocytes (A) and melanoma cells (B) are exhibited in Figure 1. The primary melanocytes isolated from C57BL/6 mice were slender with more dendrites and presented in disperse distribution. The cells took longer about 3 days to generate and would die within 10 generations. Conversely, the melanoma cells were short and full and tended to get together, conferring a significant growth advantage.

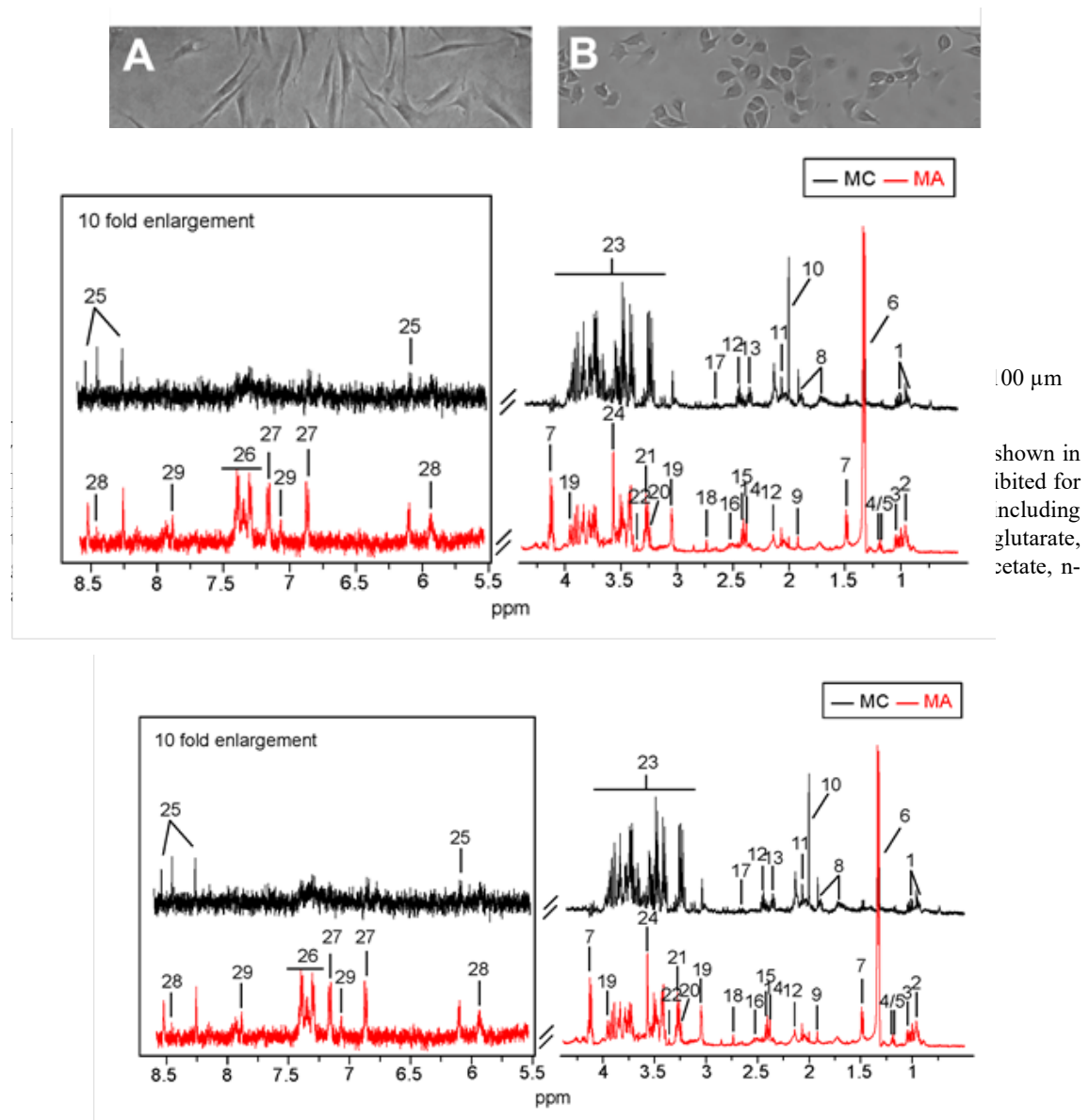


Figure 2. Typical 500 MHz ^1H NMR spectra of cell extracts obtained from melanoma cells and primary melanocytes. Metabolites: 1, Isoleucine; 2, Leucine; 3, Valine; 4, 3-Aminoisobutyrate; 5, 3-Hydroxybutyrate; 6, Lactate; 7, Alanine; 8, Lysine; 9, Acetate; 10, N-acetyl-CH₃; 11, N-acetyl cysteine; 12, Glutamine; 13, Glutamate; 14, Succinate; 15, 2-Oxoglutarate; 16, Glutathione; 17, Methionine; 18, Dimethylamine; 19, Creatine; 20, Choline; 21, Taurine; 22, Methanol; 23, Glucose; 24, Glycine; 25, ATP; 26, Phenylalanine; 27, Tyrosine; 28, Formate; 29, Histidine.

Table 1 Assignments of ¹H NMR signals for endogenous metabolites in the cells and their fold change values^b and associated p-values^c.

	Metabolites	Assignments ^a	FoldChange ^b	Pvalue ^c
1	Isoleucine	0.92(t), 1.01(d), 1.46(m),1.96(m),3.66(d)	0.98	***
2	Leucine	0.94(d), 0.96(d), 1.71(m), 3.73(m)	0.26	***
3	Valine	0.99(d), 1.04(d),2.26(m)	0.56	***
4	3-Aminoisobutyrate	1.16(d)	0.19	
5	3-Hydroxybutyrate	1.18(d)	0.63	***
6	Lactate	1.32(d), 4.12(q)	2.64	***
7	Alanine	1.48(d), 3.77(q)	1.7	***
8	Lysine	1.72(m), 1.91(m), 3.00(t), 3.76(t)	-0.79	***
9	Acetate	1.92(s)	-0.46	*
10	N-Acetyl CH ₃	2.01(s)	-2.73	***
11	N-Acetyl cysteine	2.06(s)	-1.67	***
12	Glutamine	2.16(m),2.45(m),3.77(t)	-1.19	***
13	Glutamate	2.05(m),2.34(m),3.77(t)	-1.43	***
14	Succinate	2.38(s)	0.14	
15	2-Oxoglutarate	2.42(t)	1.39	***
16	Glutathione	2.18(m), 2.55(m), 2.95(m)	0.29	**
17	Methionine	2.14(s), 2.63(t)	-1.29	***
18	Dimethylamine	2.74(s)	1.39	***
19	Creatine	3.04(s),3.93(s)	0.55	*
20	Choline	3.21(s),3.50(m),4.05(m)	-2.82	***
21	Taurine	3.26(t),3.42(t)	-1.78	***
22	Methanol	3.36(s)	-0.15	
23	Glucose	3.4-3.95 (m), 4.65(d),5.24(d)	-1.09	***
24	Glycine	3.56(s)	2.07	***
25	ATP	6.13(d),8.27(s),8.54(s)	0.06	
26	Phenylalanine	7.33(m),7.38(m),7.43(m)	0.66	***
27	Tyrosine	6.90(d),7.20(d)	1.29	***
28	Formate	8.44(s)	-1.52	***
29	Histidine	7.14 (s), 7.92 (s)	1.78	*

a Multiplicity: singlet (s), doublet (d), triplet (t), quartets (q), multiplets (m).

b Color coded according to log₂ (fold change) transformation, red indicated the increased and blue represented the decreased concentrations of metabolites extracted from melanoma cells compared to primary melanocytes.

c P-Values corrected by BH (Benjamini Hochberg) methods were calculated based on a parametric Student's t-test or a nonparametric MannWhitney test (dependent on the conformity to the normal distribution). * P < 0.05, ** P < 0.01, *** P < 0.001.



3.3 Multivariate Statistical Analysis of ¹H NMR Spectra

PCA was first applied to compare the samples spectra (Figure 3). The two groups separated clearly, suggesting that the two have disparate pathways. To search details in metabolite alterations, OPLS-DA was then performed between the two categories. The OPLS-DA score plot (Figure 4A) showed well separation similar to PCA results. And the corresponding S-plot (Figure 4B) exhibited differential metabolites modified with corresponding shapes

and colors. The more significant contributions of the metabolite to the group separation, the further distance showed from the origin. Lactate and N-acetyl-CH₃ showed the most contribution to the group distinction. Metabolic alternations were color-coded based on the correlation coefficient significance in loading plots; a red signal suggested a more important contribution to the class separation than a blue signal. Loading plots (Figure 4C and 4D) of the two groups presented concentration metabolites, including lower concentrations of lysine, acetate, n-acetyl-CH₃, n-acetyl cysteine, glutamine, glutamate, methionine, choline, taurine, glucose and formate, while isoleucine, leucine, valine, 3-hydroxybutyrate, lactate, alanine, 2-oxoglutarate, glutathione, creatine, glycine, tyrosine, phenylalanine, histidine show higher concentrations in melanoma cells. Both two-fold cross validation method testing results (Figure 4E) and 2000 times permutation test results (Figure 4F) exhibited high R², Q² and accuracy, indicating the well fitness and prediction of the model.

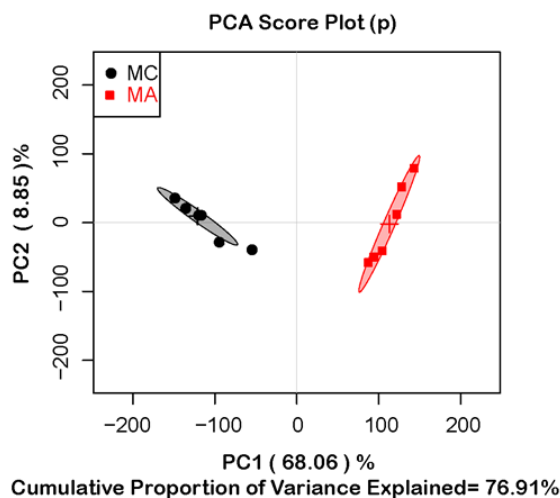


Figure 3. PCA scores plot (A) of metabolic profiles between the melanoma and primary melanocytes (n = 6). Symbols represent the primary melanocytes group (black filled circle) and melanoma group (red filled square) respectively.

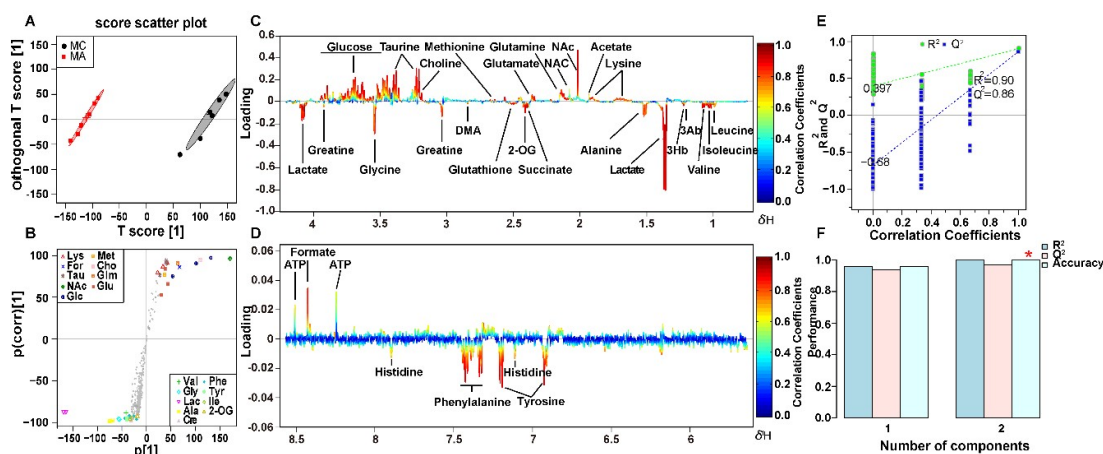


Figure 4. OPLS-DA score plot (A), S-plot (B) and color-coded coefficient loading plots (C and D), a twofold cross-validation test result (E) and the parametric result (t test) (F) based on ¹H NMR data from cerebral extracts of metabolic profiles between the melanoma cells and primary melanocytes. Metabolites that contributed to group separation were visualized and color-coded according to the absolute correlation coefficient of each variable with each group. Color was coded according to the fold change in metabolites, red indicated a more significant change than blue signals. Abbreviations: Lysine(Lys); Formate(For); Arginine(Arg); N-Acetyl CH₃(NAc); Glucose(Glc); Methonine(Met); Choline(Cho); Taurine(Tau); Glutamine(Glm); Glutamate(Glu); Valine(Val); Glycine(Gly); Lactate(Lac); Alanine(Ala); Creatine(Cre); Phenylalanine(Phe); Tyrosine(Tyr); Isoleucine(Ile); 2-Oxoglutarate(2-OG); 3-Aminoisobutyrate(3Ab); 3-Hydroxybutyrate(3Hb);

Dimethylamine(DMA); N-Acetyl cysteine(NAC).

3.4 Pathway Analysis

As showed in Table 1, the metabolites between primary melanocytes and melanoma varied a lot. Based on selected metabolites in table1, the result performed in MetPA was presented in two parts, graphical output (Figure 5) and Table S1 containing all analysis results. Disturbed pathways contained glutamine and glutamate metabolism, valine, leucine and isoleucine biosynthesis, phenylalanine, tyrosine and tryptophan metabolism, alanine, asparate and glutamate metabolism, glutathione metabolism, taurine and hypotaurine metabolism. Glutamine and glutamate metabolism is the furthest pathway from the pathway enrichment analysis and is also significant in the pathway topological analysis. According to the altered metabolites and pathway analysis, a schematic chart concerning the details was constructed (Figure 6), including glycolysis, glutaminolysis, acetate metabolism, amino acids metabolism, as well as oxidative equilibrium.

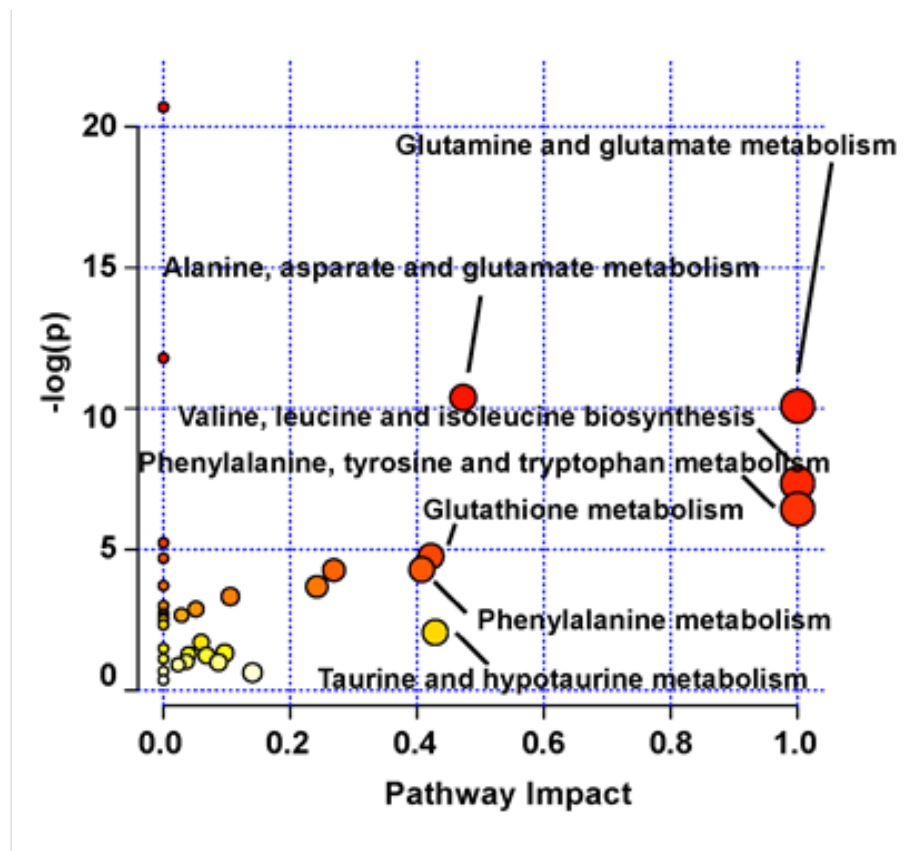


Figure 5. Bubbles plots of altered metabolic pathways in melanoma cells compared with primary melanocytes. Bubbles area was proportional to the impact of each pathway, with color denoting the significance from the highest in red to the lowest in white.

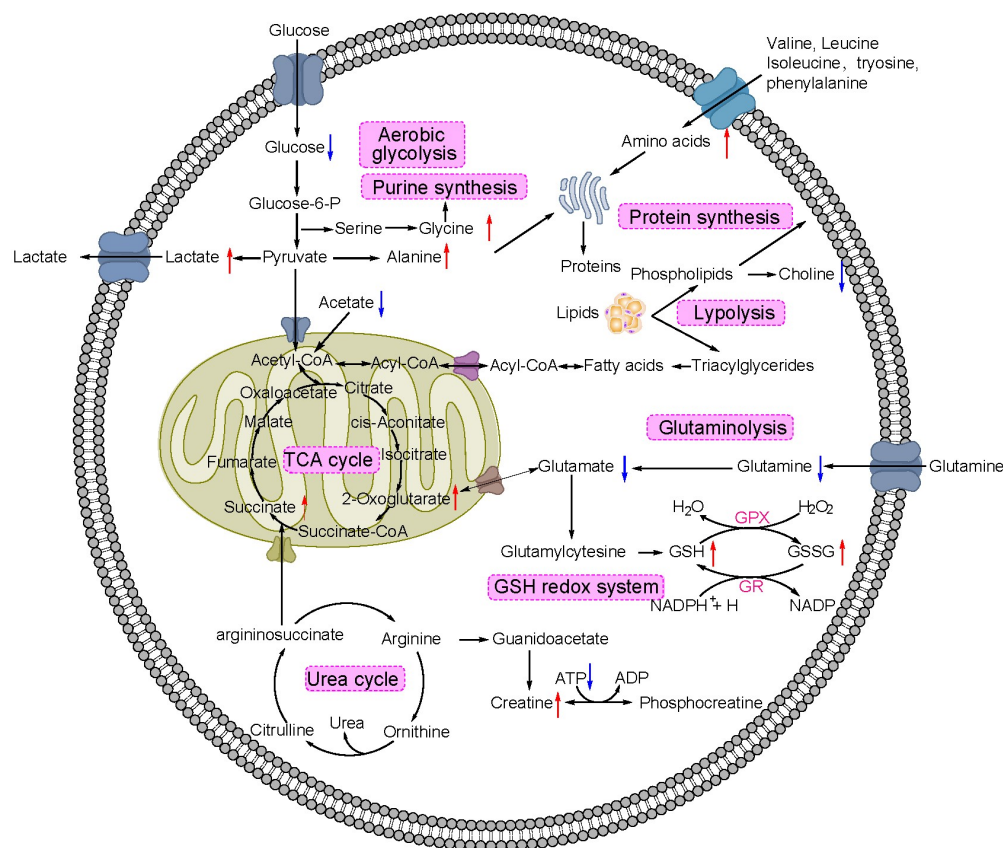


Figure 6. Schematic diagram of the perturbed metabolic pathways detected by ¹H NMR analysis showing the interrelationship of the identified metabolic pathways. Arrows (“↑↓”) in different colors represented the notable increase or decrease of metabolites in the melanoma group.

4. Discussion

The comparative approach in the research helps to demonstrate significant metabolic variances potentially linked to melanoma proliferation. Notable findings have included that the discovery of altered flux in energy metabolism containing glycolysis and glutaminolysis, disturbed amino acid metabolism and redox equilibrium were found in melanoma cells (Figure. 6).

4.1 Energy Metabolism

Under normal conditions, most mammalian cells generate energy by means of the TCA and electron transport respiratory chain in the mitochondria, with the minimal fermentation of lactate. While in tumors, upregulated glycolysis and acid resistance get a potent growth advantage in unconstrained cell populations, resulting in subsequent proliferation and invasion. As expected, the significantly decreased level of glucose and the accumulated lactate in melanoma cells showed enhanced aerobic glycolysis in figure 6, which was consistent with the Warburg effect. The increased rate of glucose uptake was directly used to support biomass accumulation and provide carbon precursors for anabolic synthesis in melanoma cells. An elevated level of lactate may promote melanoma invasion as reported (Chong et al., 2018). What’s more, increased alanine and glycine were produced from intermediates, confirming that melanoma cells prefer anabolic glycolysis for additional products.

Glutamine has been known as another energy source in tumor cells recently. Glutamine is an important mitochondrial substrate, and cells can convert glutamine-derived glutamate into 2-oxoglutarate to fuel the TCA cycle for more ATPs (Gatenby et al., 2006). What’s more, glutamine provides a nitrogen for nucleotides and amino acids biosynthesis. Evidence also showed that c-Myc oncogene is an important driver of glutamine

utilization, and its expression is important in suppressing senescence and maintaining activation of BRAF or NRAS mutations in melanoma cell lines (Son et al., 2013). The figure 5 demonstrated that glutamine and glutamate metabolism is the most significant pathway, the sharply decreased glutamine could indicate an excellent ability to switch to glutamine for production of TCA metabolites in melanoma cells, proving that melanoma relied on glutamine for growth and proliferation by glutaminolysis, as validated by elevated 2-oxoglutarate in functional TCA cycle in melanoma cells.

Choline is originated from phospholipid and a precursor of betaine (DeBerardinis & Cheng, 2010). Choline showed a disturbed manner in many cancers and has been identified as a biomarker of cell proliferation (Ueland, 2011). The decreased choline in the melanoma cells may be utilized to generate more betaine to fight against oxidative stress. Creatine and phosphocreatine played an important role in cellular energy buffering and transport (Patra et al., 2012; Ying et al., 2013). Elevated level of creatine suggested a disturbed energy metabolism in melanoma cells.

4.2 Amino Acids Metabolism

Amino acids are important metabolic regulators, and altered amino acids were highlighted in different kinds of cancers (Deminice et al., 2016; Tsun & Possemato, 2015). Many reports showed that certain amino acid transporters were up regulated in cancer, especially L-type amino acid transport (Gu et al., 2015; Ikotun et al., 2013).

Significant increase of valine, leucine and isoleucine (branched chain amino acids, BCAAs) was observed in melanoma cells. In clinic, BCAAs were used to spare protein and normalize respiratory quotients (Ohshima et al., 2016). The increased levels of BCAAs in tumor cells suggested that cells uptake more BCAAs from environment to meet demands of increased protein synthesis. Arginine is an amino acid which provides precursors for protein synthesis and intermediates in the urea cycle. Arginine was highly required in rapid growth periods like inflammation, organ dysfunction and tumor growth (Fernstrom, 2005). Melanomas were found no ability to synthesize arginine for the urea cycle enzyme arginosuccinate synthetase deficiency (Morris, 2007). The marked decreased level of arginine proved that melanoma cells were dependent on arginine called arginine auxotrophy. Thus, cell death induced by arginine deprivation is a potential cancer therapy approach to be explored in clinic (Dillon et al., 2004).

Alanine is another end point of glycolysis acted as a substrate composed of proteins. Alanine is converted from pyruvate via alanine transaminase as the standard marker of glycolytic activity in cancer cells. Alanine over output in melanoma cells is attributed to the need for excreting excess nitrogen resulting from glutamine utilization and accelerated synthesis from glucose. The result consisted with previous reports where increased production and excretion of alanine is a metabolic marker of melanoma (Filipp et al., 2012). Glycine provides two carbon atoms and a nitrogen atom in the purine biosynthesis. It is also a substrate of glutathione, which maintains intracellular redox balance mainly (Scott et al., 2011). Thus, disturbed glycine metabolism on cancer metabolomics was reported associated with constant cell proliferation (Amelio, Cutruzzolá, Antonov, Agostini, & Melino, 2014). In the study, significant increased level of glycine was shown in melanoma cells, indicating that cancer cells antagonize glycine uptake and biosynthesis to meet demands of purine production and maintain a high proliferation rate.

Tyrosine and phenylalanine are aromatic amino acids. Inefficient function of mitochondrial may cause the impaired aromatic amino acids metabolism. Increased aromatic amino acids were found in tissues of patients with gastro esophageal cancer, melanoma cells were also found with increased tyrosine and phenylalanine, revealing melanoma cells got decoupling of mitochondrial TCA activity as reported (Locasale, 2013). Moreover, melanin is formed from tyrosine, so melanoma cells absorbed more tyrosine in accordance with increased synthesis of melanin (Wiggins, Kumar, Markar, Antonowicz, & Hanna, 2015).

4.3 Redox Equilibrium

Reactive oxygen species (ROS) were regarded as a group of diatomic oxygen produced from mitochondrial electron leakage or NADPH oxidases (Krzyściak, 2011). Mitochondrial ROS contribute to the accumulation of additional mutations that promote metastatic behavior and amplify the tumorigenic phenotype. The general marker of high oxidative stress in cancer metabolism has been well recognized (Kang, Lee, & Lee, 2015). Therefore, a set of 'antioxidant' mechanisms that are expressed in various subcellular compartments are mediated to scavenge high ROS in cancer cells. The degradation of hydroperoxides is achieved initially by enzymes that supply electrons to reduce them to water. GSH redox system was commonly utilized as an antioxidant defense mechanism, where glutathione (GSH) and oxidized glutathione (GSSG) converted to each other under the control of glutathione peroxidase (GPx) and glutathione reductase (GR). The equilibrium

between the two will regulate the level of ROS in cells (Tong, Chuang, Wu, & Zuo, 2015). Elevated level of GSH has been found in many tumor cells including melanoma cells. In this study, the increased GSH indicated the activated system to regulate redox in melanoma cells, maintaining cancer cells growth advantage as reported (Carretero et al., 1999; Traverso et al., 2013).

Taurine, as the most abundant free amino acid in cells, plays several roles in essential pathways, including bile acids conjugation, membrane mobilization and maintenance of calcium homeostasis. Specially, Taurine has been reported to affect the activities and expression of antioxidant enzymes, and it has also been demonstrated that to attenuate superoxide generation by improving the function of the electron transport chain (Carretero et al., 2001). The marked low level of taurine clearly showed oxidative stress during melanoma cells growth.

5. Conclusion

In short, this is the first study to apply an NMR-based metabolomics approach to investigate the metabolic pathway variations between murine melanoma cells and primary melanocytes isolated from C57BL/6 mice. The results showed that disturbed energy metabolism, amino acid metabolism and oxidative stress in melanoma cells compared with primary melanocytes. Under the proliferation stress, the glycolytic phenotype accompanied by decreased level of glucose and abundant lactate fermentation, is necessary for evolution of invasive melanoma cells. Constitutive mobilized glutamine and lipids is likely to be an adaptation to energy demands in melanoma cells. The relatively low oxygen utilization rate in tumor cells may cause oxidative stress and mitochondria damage in cancer cells. Decreased levels of taurine and active GSH redox system indicated that they were employed to fight against the severe oxidative stress occurred in the melanoma cells. What's more, plenty of amino acids were transported for biomass during the melanoma proliferation. These evolutionary alterations effectively explain the remarkable growth advantage in melanoma cells. The study implicated that the combination of NMR technique with appropriate statistical analyses is a potent tool to identify a large number of various metabolites and depict the metabolic profiling of organisms, providing valuable information for metabolic pathway distinctions under different conditions.

References

- Amelio, I., Cutruzzolá, F., Antonov, A., Agostini, M., & Melino, G. (2014). Serine and glycine metabolism in cancer. *Trends in Biochemical Sciences*, **39**(4), 191-198.
- Andersen, L. B., Fountain, J. W., Gutmann, D. H., Tarlé, S. A., Glover, T. W., Dracopoli, N. C., . . . Collins, F. S. (1993). Mutations in the neurofibromatosis 1 gene in sporadic malignant melanoma cell lines. *Nat Genet*, **3**(2), 118-121.
- Beckonert, O., Keun, H. C., Ebbels, T. M., Bundy, J., Holmes, E., Lindon, J. C., & Nicholson, J. K. (2007). Metabolic profiling, metabolomic and metabonomic procedures for NMR spectroscopy of urine, plasma, serum and tissue extracts. *Nat Protoc*, **2**(11), 2692-2703.
- Cairns, R. A., Harris, I. S., & Mak, T. W. (2011). Regulation of cancer cell metabolism. *Nat Rev Cancer*, **11**(2), 85-95.
- Cantor, J. R., & Sabatini, D. M. (2012). Cancer cell metabolism: one hallmark, many faces. *Cancer Discov*, **2**(10), 881-898.
- Carretero, J., Obrador, E., Anasagasti, M. J., Martin, J. J., Vidal-Vanaclocha, F., & Estrela, J. M. (1999). Growth-associated changes in glutathione content correlate with liver metastatic activity of B16 melanoma cells. *Clin Exp Metastasis*, **17**(7), 567-574.
- Carretero, J., Obrador, E., Esteve, J. M., Ortega, A., Pellicer, J. A., Sempere, F. V., & Estrela, J. M. (2001). Tumoricidal activity of endothelial cells. Inhibition of endothelial nitric oxide production abrogates tumor cytotoxicity induced by hepatic sinusoidal endothelium in response to B16 melanoma adhesion in vitro. *J Biol Chem*, **276**(28), 25775-25782.
- Chong, J., Soufan, O., Li, C., Caraus, I., Li, S., Bourque, G., . . . Xia, J. (2018). MetaboAnalyst 4.0: towards more transparent and integrative metabolomics analysis. *Nucleic Acids Res*, **46**(W1), W486-w494.
- Cillo, C., Dick, J. E., Ling, V., & Hill, R. P. (1987). Generation of drug-resistant variants in metastatic B16 mouse melanoma cell lines. *Cancer Res*, **47**(10), 2604-2608.
- Colombino, M., Capone, M., Lissia, A., Cossu, A., Rubino, C., De Giorgi, V., . . . Palmieri, G. (2012).

- BRAF/NRAS mutation frequencies among primary tumors and metastases in patients with melanoma. *J Clin Oncol*, **30**(20), 2522-2529.
- Cui, Q., Lewis, I. A., Hegeman, A. D., Anderson, M. E., Li, J., Schulte, C. F., . . . Markley, J. L. (2008). Metabolite identification via the Madison Metabolomics Consortium Database. *Nat Biotechnol*, **26**(2), 162-164.
- Cuperlovic-Culf, M., Ferguson, D., Culf, A., Morin, P., Jr., & Touaibia, M. (2012). 1H NMR metabolomics analysis of glioblastoma subtypes: correlation between metabolomics and gene expression characteristics. *J Biol Chem*, **287**(24), 20164-20175.
- Curtin, J. A., Fridlyand, J., Kageshita, T., Patel, H. N., Busam, K. J., Kutzner, H., . . . Bastian, B. C. (2005). Distinct sets of genetic alterations in melanoma. *N Engl J Med*, **353**(20), 2135-2147.
- De Meyer, T., Sinnaeve, D., Van Gasse, B., Tsiporkova, E., Rietzschel, E. R., De Buyzere, M. L., . . . Van Criekinge, W. (2008). NMR-based characterization of metabolic alterations in hypertension using an adaptive, intelligent binning algorithm. *Anal Chem*, **80**(10), 3783-3790.
- DeBerardinis, R. J., & Cheng, T. (2010). Q's next: the diverse functions of glutamine in metabolism, cell biology and cancer. *Oncogene*, **29**(3), 313-324.
- Deminice, R., Cella, P. S., Padilha, C. S., Borges, F. H., da Silva, L. E., Campos-Ferraz, P. L., . . . Guarnier, F. A. (2016). Creatine supplementation prevents hyperhomocysteinemia, oxidative stress and cancer-induced cachexia progression in Walker-256 tumor-bearing rats. *Amino Acids*, **48**(8), 2015-2024.
- Dillon, B. J., Prieto, V. G., Curley, S. A., Ensor, C. M., Holtsberg, F. W., Bomalaski, J. S., & Clark, M. A. (2004). Incidence and distribution of argininosuccinate synthetase deficiency in human cancers: a method for identifying cancers sensitive to arginine deprivation. *Cancer*, **100**(4), 826-833.
- Fedele, T. A., Galdos-Riveros, A. C., Jose de Farias e Melo, H., Magalhães, A., & Maria, D. A. (2013). Prognostic relationship of metabolic profile obtained of melanoma B16F10. *Biomed Pharmacother*, **67**(2), 146-156.
- Feng, J., Isern, N. G., Burton, S. D., & Hu, J. Z. (2013). Studies of Secondary Melanoma on C57BL/6J Mouse Liver Using 1H NMR Metabolomics. *Metabolites*, **3**(4), 1011-1035.
- Fernstrom, J. D. (2005). Branched-chain amino acids and brain function. *J Nutr*, **135**(6 Suppl), 1539s-1546s.
- Filipp, F. V., Ratnikov, B., De Ingeniis, J., Smith, J. W., Osterman, A. L., & Scott, D. A. (2012). Glutamine-fueled mitochondrial metabolism is decoupled from glycolysis in melanoma. *Pigment Cell Melanoma Res*, **25**(6), 732-739.
- Gatenby, R. A., & Gawlinski, E. T. (1996). A reaction-diffusion model of cancer invasion. *Cancer Res*, **56**(24), 5745-5753.
- Gatenby, R. A., Gawlinski, E. T., Gmitro, A. F., Kaylor, B., & Gillies, R. J. (2006). Acid-mediated tumor invasion: a multidisciplinary study. *Cancer Res*, **66**(10), 5216-5223.
- Gordon, P. R., Mansur, C. P., & Gilchrist, B. A. (1989). Regulation of human melanocyte growth, dendricity, and melanization by keratinocyte derived factors. *J Invest Dermatol*, **92**(4), 565-572.
- Gu, Y., Chen, T., Fu, S., Sun, X., Wang, L., Wang, J., . . . Wang, M. (2015). Perioperative dynamics and significance of amino acid profiles in patients with cancer. *J Transl Med*, **13**, 35.
- Ikotun, O. F., Marquez, B. V., Huang, C., Masuko, K., Daiji, M., Masuko, T., . . . Lapi, S. E. (2013). Imaging the L-type amino acid transporter-1 (LAT1) with Zr-89 immunoPET. *PLoS One*, **8**(10), e77476.
- Kang, S. W., Lee, S., & Lee, E. K. (2015). ROS and energy metabolism in cancer cells: alliance for fast growth. *Arch Pharm Res*, **38**(3), 338-345.
- Kim, H. Y., Lee, H., Kim, S. H., Jin, H., Bae, J., & Choi, H. K. (2017). Discovery of potential biomarkers in human melanoma cells with different metastatic potential by metabolic and lipidomic profiling. *Sci Rep*, **7**(1), 8864.
- Krzyściak, W. (2011). Activity of selected aromatic amino acids in biological systems. *Acta Biochim Pol*, **58**(4), 461-466.
- Lakhter, A. J., Hamilton, J., Konger, R. L., Brustovetsky, N., Broxmeyer, H. E., & Naidu, S. R. (2016). Glucose-independent Acetate Metabolism Promotes Melanoma Cell Survival and Tumor Growth. *J Biol Chem*, **291**(42), 21869-21879.

- Li, M. H., Ruan, L. Y., Chen, C., Xing, Y. X., Hong, W., Du, R. H., & Wang, J. S. (2018). Protective effects of *Polygonum multiflorum* on ischemic stroke rat model analysed by (1)H NMR metabolic profiling. *J Pharm Biomed Anal*, **155**, 91-103.
- Locasale, J. W. (2013). Serine, glycine and one-carbon units: cancer metabolism in full circle. *Nat Rev Cancer*, **13**(8), 572-583.
- Morris, S. M., Jr. (2007). Arginine metabolism: boundaries of our knowledge. *J Nutr*, **137**(6 Suppl 2), 1602s-1609s.
- Ohshima, Y., Kaira, K., Yamaguchi, A., Oriuchi, N., Tominaga, H., Nagamori, S., . . . Ishioka, N. S. (2016). Efficacy of system I amino acid transporter 1 inhibition as a therapeutic target in esophageal squamous cell carcinoma. *Cancer Sci*, **107**(10), 1499-1505.
- Olivares, O., Däbritz, J. H. M., King, A., Gottlieb, E., & Halsey, C. (2015). Research into cancer metabolomics: Towards a clinical metamorphosis. *Semin Cell Dev Biol*, **43**, 52-64.
- Patra, S., Ghosh, A., Roy, S. S., Bera, S., Das, M., Talukdar, D., . . . Ray, M. (2012). A short review on creatine-creatine kinase system in relation to cancer and some experimental results on creatine as adjuvant in cancer therapy. *Amino Acids*, **42**(6), 2319-2330.
- Scott, D. A., Richardson, A. D., Filipp, F. V., Knutzen, C. A., Chiang, G. G., Ronai, Z. A., . . . Smith, J. W. (2011). Comparative metabolic flux profiling of melanoma cell lines: beyond the Warburg effect. *J Biol Chem*, **286**(49), 42626-42634.
- Sinclair, A. J., Viant, M. R., Ball, A. K., Burdon, M. A., Walker, E. A., Stewart, P. M., . . . Young, S. P. (2010). NMR-based metabolomic analysis of cerebrospinal fluid and serum in neurological diseases--a diagnostic tool? *NMR Biomed*, **23**(2), 123-132.
- Son, J., Lyssiotis, C. A., Ying, H., Wang, X., Hua, S., Ligorio, M., . . . Kimmelman, A. C. (2013). Glutamine supports pancreatic cancer growth through a KRAS-regulated metabolic pathway. *Nature*, **496**(7443), 101-105.
- Tong, L., Chuang, C. C., Wu, S., & Zuo, L. (2015). Reactive oxygen species in redox cancer therapy. *Cancer Lett*, **367**(1), 18-25.
- Traverso, N., Ricciarelli, R., Nitti, M., Marengo, B., Furfaro, A. L., Pronzato, M. A., . . . Domenicotti, C. (2013). Role of glutathione in cancer progression and chemoresistance. *Oxid Med Cell Longev*, **2013**, 972913.
- Tsun, Z. Y., & Possemato, R. (2015). Amino acid management in cancer. *Semin Cell Dev Biol*, **43**, 22-32.
- Ueland, P. M. (2011). Choline and betaine in health and disease. *J Inherit Metab Dis*, **34**(1), 3-15.
- Vander Heiden, M. G., Cantley, L. C., & Thompson, C. B. (2009). Understanding the Warburg effect: the metabolic requirements of cell proliferation. *Science*, **324**(5930), 1029-1033.
- Wang, X., Hu, M., Feng, J., Liu, M., & Hu, J. Z. (2014). (1)H NMR Metabolomics Study of Metastatic Melanoma in C57BL/6J Mouse Spleen. *Metabolomics*, **10**(6), 1129-1144.
- Warburg, O., Wind, F., & Negelein, E. (1927). THE METABOLISM OF TUMORS IN THE BODY. *J Gen Physiol*, **8**(6), 519-530.
- Wiggins, T., Kumar, S., Markar, S. R., Antonowicz, S., & Hanna, G. B. (2015). Tyrosine, phenylalanine, and tryptophan in gastroesophageal malignancy: a systematic review. *Cancer Epidemiol Biomarkers Prev*, **24**(1), 32-38.
- Wishart, D. S. (2016). Emerging applications of metabolomics in drug discovery and precision medicine. *Nat Rev Drug Discov*, **15**(7), 473-484.
- Wishart, D. S., Jewison, T., Guo, A. C., Wilson, M., Knox, C., Liu, Y., . . . Scalbert, A. (2013). HMDB 3.0--The Human Metabolome Database in 2013. *Nucleic Acids Res*, **41**(Database issue), D801-807.
- Xing, Y. X., Li, M. H., Tao, L., Ruan, L. Y., Hong, W., Chen, C., . . . Wang, J. S. (2018). Anti-Cancer Effects of Emodin on HepG2 Cells as Revealed by (1)H NMR Based Metabolic Profiling. *J Proteome Res*, **17**(5), 1943-1952.
- Ying, J., Rahbar, M. H., Hallman, D. M., Hernandez, L. M., Spitz, M. R., Forman, M. R., & Gorlova, O. Y. (2013). Associations between dietary intake of choline and betaine and lung cancer risk. *PLoS One*, **8**(2), e54561.
- Zaidi, N., Lupien, L., Kuemmerle, N. B., Kinlaw, W. B., Swinnen, J. V., & Smans, K. (2013). Lipogenesis and lipolysis: the pathways exploited by the cancer cells to acquire fatty acids. *Prog Lipid Res*, **52**(4), 585-589.